

Consequences of kinetic inhomogeneities in glasses

Donna N. Perera* and Peter Harrowell†

School of Chemistry, University of Sydney, New South Wales 2006, Australia

(Received 14 December 1995)

Many of the physical pictures used to rationalize the phenomenology of glassy dynamics rest upon a consideration of spatial fluctuations in the relaxation kinetics of the glass-forming liquid. We examine the wide ranging consequences which flow from assuming the existence of transient kinetic inhomogeneities. These consequences include: strong and fragile behavior, two-step relaxation processes, nonlinear relaxation following temperature jumps, spatially correlated kinetics and non-Gaussian behavior of incoherent processes. These general predictions are explored in simulations in which relaxation is governed by diffusing defects. [S1063-651X(96)07008-0]

PACS number(s): 61.43.Fs, 64.70.Pf, 66.10.Cb, 78.35.+c

I. INTRODUCTION

The theoretical description and experimental characterization of the collective dynamics of glass-forming liquids remains the central problem posed by the glassy state. The ubiquity of glassy dynamics leads us to expect that the major features of this relaxation can be described without explicit reference to specific molecular interactions or internal degrees of freedom. In this paper we examine a description of cooperative dynamics which focuses on the spatial correlation and dynamics of the transient distribution of local relaxation times in the glass-forming liquid. For a simple model glass [1–4], we have recently demonstrated that a number of characteristic features including non-Arrhenius temperature dependence of relaxation times, stretched exponential relaxation, and nonlinear behavior following temperature jumps are the result of the transient spatial inhomogeneities of the relaxation process. These fluctuations arise from the strong dependence of the local relaxation time on local configurations. Their presence is *inevitable* in any system probed on time scales shorter than the structural relaxation time—a defining feature of glass experiments. What remains to be established is whether or not these fluctuations play the same central role in the relaxation of *real* materials as they do in the simulated models.

Our goal in this paper is to present the wide range of physical consequences which flow from a quite general assumption concerning the existence of kinetic inhomogeneities. While some of these consequences are already well established in the literature in connection with specific models, we shall argue that many of these features are independent of the details of the models with which they are associated. This work is motivated by a belief that the recognition of the central role that kinetic inhomogeneities play in many theoretical models of glassy relaxation is both useful and little appreciated. By establishing the generic consequences arising from the existence of such transient distribution, we would also like to identify explicit tests (by experiment or

simulation) of the relevance of these inhomogeneities to real glasses.

II. BACKGROUND

The proposal that glassy relaxation reflects spatial inhomogeneities has a long history. Glass theories based on the existence of a thermodynamic singularity [5–7] have, either explicitly or implicitly, accounted for the glassy dynamics in terms of the kinetics of the clusters of the new phase. In the language of kinetic inhomogeneities, such cluster models focus on the localization of the particles undergoing slow relaxation. On the other hand, it is the fast regions which constitute the localized objects in free volume [8] and diffusing defect models [9–12]. A number of authors [13] have explored models based on fluctuations in local bond numbers. These models, along with a number of recent lattice models of glasses [14], underline the role of local environments in establishing the local dynamics through short range interactions. The spatial distribution of relaxation times in such models is typically a nonlinear and nonlocal (in time and/or space) function of the local environment fluctuations. The central role played by inhomogeneous kinetics is made explicit in “two-fluid” models proposed recently [15–17] where the cooperative dynamics is characterized by slow and fast subpopulations of particles. All these theoretical approaches have focused on different explanations of the distribution of relaxation rates. We argue here that the consequences of the spatial inhomogeneities themselves (the common feature of all the models mentioned) have not been fully explored.

The idea of heterogeneous kinetics figures prominently in the physical interpretation of a number of important experiments. Johari and Goldstein [18] invoked localized fast domains in accounting for the relaxation of intermediate frequency, processes these authors labeled as β , distinguishing them from the long time relaxation α . Cavaille, Perez, and Johari [19] have developed a heterogeneous model of the rheology of glasses. The fact that slow and fast relaxation are associated with different particle subpopulations has been established for some polymer systems by Spiess and co-workers [20] using an elegant four dimensional (4D) nuclear magnetic resonance (NMR) experiment. Cicerone and Ediger

*Electronic address: perer@d@chem.usyd.edu.au

†Electronic address: peter@chem.usyd.edu.au

[21] have also shown, via selective photobleaching of probe molecules, that there exists a long-lived distribution of mobilities in supercooled ortho-terphenyl. This kinetic differentiation of particles, which persisted for times of the order of the structural relaxation, is termed “heterogeneous relaxation.” Sillescu *et al.* [16] have established the surprising result that the translational diffusion constant of molecular probes in ortho-terphenyl apparently decreases more slowly with decreasing temperature, at large supercooling, than does the rotational diffusion constant. These authors propose that the formation of fast localized aggregates that decay on the time scale of the structural relaxation time may account for this observation. A number of alternative explanations of these measurements have been developed [15,17,22] around the general idea that translational motion averages over a spatially varying environment quite differently from rotational motion. As a final example, it has been recently suggested [23] that kinetic inhomogeneities are responsible for the deviation of crystallization kinetics at large supercoolings in lithium disilicate from that described by classical nucleation theory. The idea is that nucleation is effectively restricted to the fast regions. In fragile liquids it is the scarcity of these regions, rather than the probability of crystalline fluctuations, which comes to dominate the rate of crystal formation.

The paper is organized as follows. In the next section we describe, qualitatively, the consequences arising from general considerations of the inhomogeneous picture. While the results of Sec. III stand on their own, they give little indication of the magnitude of the effects described. To examine this quantitative question, we present an explicit model of glassy relaxation involving the simulation of relaxation mediated by diffusing defects whose waiting times obey an algebraic distribution as described by Shlesinger and Montroll [10]. Details of the calculations are provided in Sec. IV. In Sec. V we present the results of the simulations in the form of relaxation functions and their scaling, the relationship between fragility and the stretching of the relaxation, the nonlinear response following temperature jumps, and the spatial distribution of the kinetic processes in strong and fragile fluids. We conclude with a discussion.

III. CONSEQUENCES OF KINETIC INHOMOGENEITIES

We shall consider a bimodal distribution of local environments, characterized as “slow” and “fast,” in a dense material. Such a picture implies *at least* two characteristic temperatures, one to establish a time scale and another to determine the distribution of slow and fast environments. Let the relaxation time in a fast region be given by $\tau_j = \tau_j(T/T_1)$, where T is the temperature and T_1 is the characteristic temperature of this fast kinetics. We shall assume that the kinetics of the slow regions is so much slower than in the fast regions that it does not contribute to relaxation. Instead, relaxation takes place by the exchange of environments between the slow and the fast. This exchange is a complex process and is the origin of the complex dynamics. For simplicity, let $C(T/T_h)$ be the volume fraction of fast regions, a decreasing function of T , with T_h the single characteristic temperature of this volume fraction. (The following analysis does not depend crucially on this assumption of a

single characteristic temperature for C .) The following features arise as consequences of this minimal picture.

(1) *Strong and fragile behavior.* The overall relaxation time τ is given by

$$\tau(T) = \tau_f(T/T_1)f(T/T_h), \quad (1)$$

where $f(T/T_h)$ is proportional to the time scale of the environment exchange process and is expected to be a decreasing function of C , approaching one from above as C approaches one. Results of both the facilitated kinetic Ising model [1] and the diffusing defect model [12] indicate that $f(T/T_h)$ is proportional to $C^{-\lambda}$ where $\lambda > 1$. The relaxation time is governed by these two temperatures. If $T_1 \gg T_h$ then, over the accessible time scales, $f(T/T_h)$ remains at its higher temperature value (i.e., $\lim_{T \rightarrow \infty} f = 1$) and the temperature dependence is determined by that of the relaxation time in the fast regions. Given that this relaxation takes place, by definition, without the need for any extended cooperativity, we can assume that τ_f has an Arrhenius temperature dependence. Hence a liquid characterized by the above inequality would resemble a *strong* liquid. Conversely, if $T_1 \ll T_h$ the relaxation time is dominated by the exchange of the slow and fast environments which, as a result of the complex extended correlations in such dynamics, is typically non-Arrhenius. We shall regard this as a *fragile* liquid.

This picture of fragility is of immediate relevance to experiments in restricted geometries and to computer simulations of glasses in general. As the temperature drops and the equilibrium density of fast environments decreases, the average distance between these mobile regions eventually becomes of the order of the system itself. At this point we expect to see in fragile liquids (but not in strong liquids) a system size dependence of the relaxation time—the signature of the growth of the cooperative length scale. While this observation is commonplace in studies of lattice models of glass formers [1,14,24], we are not aware of any reports of such a size dependence in simulations of models with continuous degrees of freedom.

(2) *The relaxation function is the sum of the contributions from different environments.* Central to this picture is the idea that fast and slow dynamics arise from different transient subpopulations of particles. It follows directly that “caging,” defined as the transient localization of individual particles, is a feature of a subpopulation of the particles only. The relaxation function has the general form

$$\phi(t) = C \phi_f(t/\tau_f) + (1 - C) \phi_h(t/\tau), \quad (2)$$

reflecting the different relaxation processes. Relaxation in the fast region is assumed to be exponential (although, in general, this is not necessary). $\phi_h(t/\tau)$ describes the exchange process throughout the medium and will extend over a stretched range of time scales. The *a priori* calculation of a function like $\phi_h(t/\tau)$ is an important goal of a glass theory. Our aim here is more modest—to identify generic features of inhomogeneous relaxation in order to learn more about the nature of the exchange between different local configurations. Such insights would provide us with a deeper physical understanding of the origins of $\phi_h(t/\tau)$. The fast fraction C establishes the fraction of the system relaxed by the short time processes, i.e., the *amplitude* of the fast relaxation pro-

cess. In fragile liquids, C also establishes the relaxation time for the slow process [specific examples of the relationship between C and τ are mentioned in point (1)]. These two different types of scaling have been explicitly demonstrated for the facilitated kinetic Ising model [4] but we are unaware of any other tests of its validity. We shall return to this feature in Sec. V.

(3) *A positive correlation between stretched relaxation and fragility.* As, in this picture, both stretched relaxation and fragility are characteristic of kinetics dominated by environment exchange processes, the inhomogeneous picture implies a generally positive correlation between these two features. This correlation is certainly consistent with the compilation of data presented by Böhmer *et al.* [25]. We cannot conclude, however, that a linear or, even, monotonic relation between any specific measures of stretched relaxation and fragility follows as an immediate consequence of the inhomogeneous picture. As the fragility increases, slower components of the environment exchange process begin to play a significant role in relaxation. The observed width of the relaxation process will reflect the subtleties of the particular sampling of the complex dynamics of the local environments. In Sec. V, we shall examine the details of this correlation between fragility and relaxation in the diffusing defect model.

(4) *Nonlinear response and the relaxation of kinetic environments.* An important body of data on glassy relaxation is based on the transient response of various properties (e.g., viscosity, heat capacity, thermal expansion coefficient) of the glass former to temperature jumps [26]. A characteristic feature common to a wide range of fragile glass formers is a dependence of the relaxation on the sign and magnitude of the temperature change ΔT . The relaxation time, in such systems, is itself relaxing in time—a classic example of a nonlinear effect. As thermal conductivity is one of the few transport coefficients which shows no significant slowing down near the glass transition, the time dependence of establishing the new temperature throughout the material can be neglected. As a result we can assume that τ_f equilibrates to the new temperature instantaneously. The volume fraction of fast environments C , however, has to relax to the new equilibrium value over some finite time scale, and this time scale will, of course, depend on C itself. The lag between the actual value of C and the equilibrium value is a measure of the configurational nonequilibrium during the temperature jump transient. The quantity C plays a similar conceptual role to the fictive temperature which, in work by Moynihan *et al.* [27] and Hodge [28], has proven an elegant tool in correlating linear and nonlinear relaxation. As the nonlinear behavior is described here as arising from the role of the inhomogeneities, we expect strong liquids to show less nonlinearity than fragile liquids. Further we expect relaxation at a temperature T following a temperature *increase* to be slower than relaxation at T following a temperature *decrease*. This prediction is a reflection of the different densities of fast regions at the respective initial temperatures. This asymmetry in relaxation behavior has been observed experimentally [29] and in simulations of the facilitated kinetic Ising model [30]. In Sec. V we calculate the magnitude of the asymmetric response of the relaxation following tem-

perature jumps of the diffusing defect model, generalized to include defect production and annihilation.

The very picture of a long-lived inhomogeneous distribution of relaxation times resulting from the equilibrium structural fluctuations implies that relaxation involves the coupling of modes. Consider the relaxation by diffusion of a particular Fourier mode of a density fluctuation. Under linear diffusion, each mode relaxes independently of other density modes. A spatially dependent diffusion constant, however, couples the dynamics of mode with different wave vectors. The possibility that such a coupling could have interesting and observable effects in glasses has been explored in a recent study [22].

(5) *Spatial correlations and characteristic length scales of the transient kinetic structure.* We note that, while the inhomogeneous picture itself does not specify any particular correlations between the slow and fast regions, specification of a mechanism for exchange between these environments will impose certain spatial correlations. If relaxation is restricted to the fast regions then so must this environment exchange. It follows that cooperative relaxation processes must proceed by the complex “motion” of fast environments throughout the material. The local relaxation time of a particle will then depend on its proximity to a fast region. The slowest regions, responsible for the long time tail of the relaxation process, will tend to be clumped together in those regions of volume maximally distanced from all fast regions at some initial time. It is interesting that we have arrived at such a correlation, which resembles that of the cluster models (i.e., localized domains of slow relaxation), from a general kinetic argument rather than having to speculate on specific equilibrium fluctuations. An experiment which could resolve the spatial correlations of relaxation times would be able to test for such kinetic structure. No such experiment currently exists. This kinetic structure has been observed in simulations of the facilitated kinetic Ising model [1,3], a 3D lattice model of a simple liquid [31], and in molecular dynamic simulations of a 2D liquid [32].

(6) *Non-Gaussian behavior of incoherent processes.* While many fundamental problems remain concerning single particle dynamics and stress relaxation in the presence of fluctuating inhomogeneities, we can offer a general observation concerning the consequences of kinetic structure. Single particle motion is expected to exhibit a long-lived non-Gaussian character. By way of example, consider a simple model in which each particle starts off in an environment characterized by a particular diffusion constant and, over some time period, eventually samples all possible environments. It can be easily shown that the non-Gaussian parameter $A(t)$ defined as

$$A(t) = \frac{3\langle \Delta r(t)^4 \rangle}{5\langle \Delta r(t)^2 \rangle^2} - 1, \quad (3)$$

where $\langle \Delta r(t)^2 \rangle$ is the mean squared displacement and $\langle \Delta r(t)^4 \rangle$ the mean quartic displacement, can only approach zero (and hence Gaussian behavior) for times exceeding the time scale required for individual particles to sample the complete distribution of kinetic environments. The decay of $A(t)$ then, provides us with an upper bound on a “mixing time” similar to that discussed in Refs. [20] and [21]. De-

viations from Gaussian behavior have been observed in a number of simulations of glass forming systems [33,34]. An analysis of $A(t)$ in terms of kinetic inhomogeneities is presented elsewhere [35].

IV. SIMULATION OF THE DEFECT DIFFUSION MODEL: BACKGROUND AND COMPUTATIONAL DETAILS

The consequences of inhomogeneous relaxation described above follow directly from the assumption of kinetic inhomogeneities. They are, however, qualitative in nature, providing little in the way of quantitative estimates. To go beyond these general observations we must look at specific models. In this spirit, we present simulations of dielectric relaxation governed by diffusing defects. A brief background to this model and the details of the calculation are presented in this section.

A defect diffusion model of dielectric relaxation was first introduced by Glarum [9] in 1960. It was proposed that the reorientation of a dipole occurred as soon as a defect diffused to the site of the dipole. Glarum showed that in 1D this model gave a stretched exponential dielectric relaxation, similar to that seen experimentally. Bordewijk [36], in 1975, applied a similar model to relaxation in 3D only to find the long time relaxation decayed via a simple exponential process. With this failure to model glassy relaxation in 3D, the model languished until Shlesinger and Montroll [10] demonstrated that stretched exponential relaxation could be recovered in 3D if the defect motion was characterized by an algebraic waiting time distribution (as opposed to the exponential distributions assumed by Glarum and Bordewijk). In subsequent papers, Bendler and Schlesinger [11,12] applied this model to the problem of glassy kinetics, drawing heavily on asymptotic analysis of the relaxation function. To our knowledge, however, the model has not been previously studied by numerical simulation.

The stimulated system consist of a cubic lattice of dimensions $100 \times 100 \times 100$ lattice spacings. Each defect occupies a finite spherical volume of radius one lattice spacing l and is free to move off lattice. Initially the defects are randomly distributed in the simulation box. The defects are allowed to jump a fixed length l in any direction and are permitted to overlap one another (i.e., we neglect any defect-defect interaction). The defect concentration,

$$C_D = N_D / V, \quad (4)$$

where N_D is the number of defects and V is the total number of lattice sites, remains constant during a simulation run.

The waiting time distribution of the defects is given by

$$\Psi(t) = \alpha t_{\min}^{\alpha} t^{-1-\alpha}, \quad (5)$$

where t_{\min} is the short time cutoff of the distribution and the exponent α is selected from the range $0 < \alpha \leq 1$. It follows directly from Eq. (5) that the mean waiting time between jumps for a given defect is infinite. This lack of a characteristic time scale associated with the hopping process has resulted in its description as ‘‘fractal’’ and leads to stretched exponential relaxation. We use the distribution in Eq. (5) in this paper (without any *a priori* justification) to provide a

simple model of the kinetic consequences of the complex dynamics associated with environment exchange.

In order to simulate dielectric relaxation, we assign each site i on the lattice with a state σ_i which can take on one of two values $\sigma_i = 0$ or $\sigma_i = 1$ depending on whether the site is in a relaxed or unrelaxed state, respectively. Initially all σ_i 's are set to 1, i.e., all sites are in an unrelaxed state. We assume that the instantaneous relaxation of a site occurs with probability

$$p(t) = 1 - \exp(-t/t_{\min}), \quad (6)$$

when it lies within a single lattice spacing from the center of a defect with waiting time t . Note that the choice of $p(t)$ in Eq. (6) is equivalent to assuming exponential relaxation within a fast region. The time scale t_{\min} is equivalent to τ_f from the previous discussion and so we assume that its temperature dependence is Arrhenius, i.e.,

$$t_{\min} = t_0 \exp(T_1 / T). \quad (7)$$

The choice of the temperature dependence of the defect concentration C_D remains. Here we have set

$$C_D = C_D^0 \exp\left[\frac{-B}{(T - T_0)^{1.5}}\right], \quad (8)$$

chosen explicitly so that the model will reasonably mimic the temperature dependence of a range of fragile liquids over a restricted temperature range. We *do not* mean to imply that there is necessarily a nonzero temperature at which mobile fast environments will vanish. This specific form comes from Bendler and Shlesinger [11]. We note that this temperature dependence of the generalized Vogel-Fulcher form requires two characteristic temperatures, as opposed to the single T_h used in the preceding section. The temperature independent prefactor C_D^0 allows us to ‘‘fit’’ the defect density into the range available to our simulations. In the simulations the defect density is bounded from below as we cannot drop to a density below one defect in the simulation cell. For the system size used here that density is 10^{-6} defects per lattice site.

The relaxation of the system is monitored through the function

$$\phi(t) = N_{\sigma=1}(t) / V, \quad (9)$$

where $N_{\sigma=1}$ is the number of sites for which $\sigma_i = 1$ (i.e., the number of unrelaxed sites) and V is defined as above. $\phi(t)$ is then the fraction of unrelaxed sites at time t . A relaxation time τ is defined as the area under $\phi(t)$.

In summary, a simulation run consists of spherical, non-interacting, ‘‘ghostlike’’ defects of fixed volume undergoing an off-lattice random walk. All defects are assigned a waiting time according to the distribution $\Psi(t)$ in Eq. (5). Only when a defect's waiting time expires, is it allowed to take a jump of fixed length in any direction. Hence the defect with the shortest waiting time jumps first. It is then assigned a new waiting time and the system is advanced in time to the next jump. Each time a defect overlaps a site, it has a probability $p(t)$ in Eq. (6) of relaxing that site. The diffusive motion of the defects is activated only above t_{\min} . For

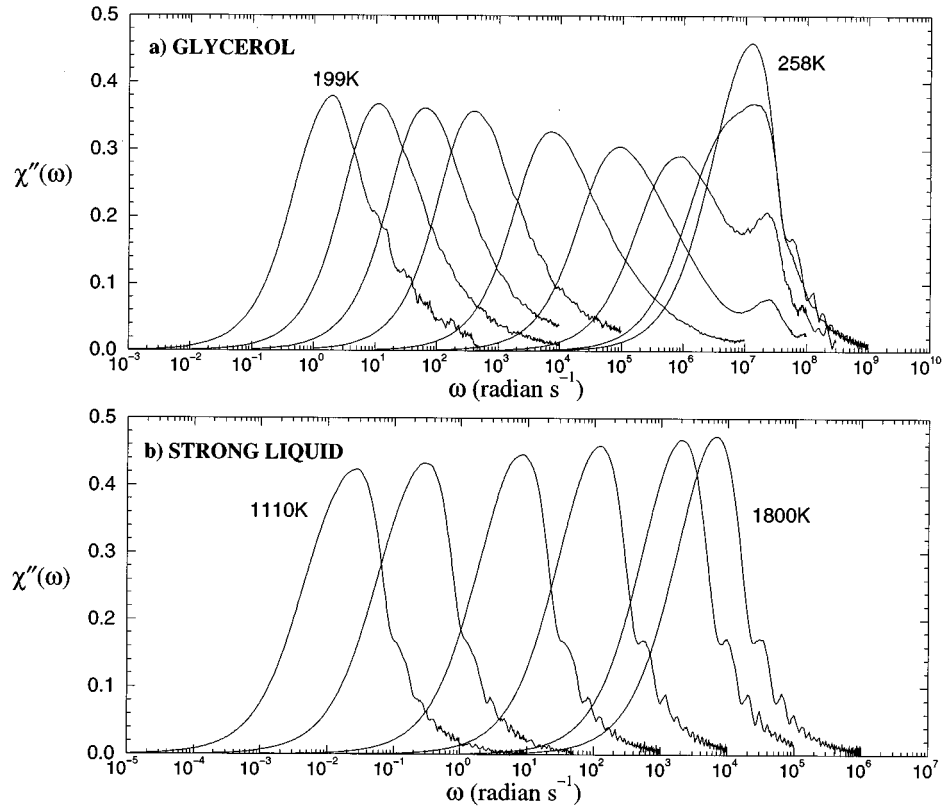


FIG. 1. (a) The susceptibility spectrum $\chi''(\omega)$ as a function of angular frequency ω for a system modeled with “glycerol” parameters (Sec. V A). The temperatures of the curves from left to right are 199, 203, 208, 213, 223, 233, 243, 253, and 258 K, respectively. The experimental glass transition temperature $T_g = 193$ K [37]. Note the distinct low frequency (α) peak whose position exhibits a striking temperature dependence. At higher temperatures, a high frequency (β) peak appears with a peak position which shows little variation with temperature due to the constraint of constant t_{\min} . (b) The susceptibility spectrum for a system modeled as a “strong liquid” with parameters as in (a) above, except that $RT_1 = 300$ kJ mol^{-1} and t_{\min} is now temperature dependent. The temperature of the curves from left to right are 1110, 1200, 1350, 1500, 1700, and 1800 K, respectively. $T_g = 1110$ K, the temperature at which $\tau = 100$ s. Only a single β peak whose width decreases with increasing temperature is observed.

$t \leq t_{\min}$, the system is assumed to relax exponentially according to Eq. (6), that is the fraction of relaxed sites is given by

$$1 - \phi(t) = p(t)C_0 \quad 0 \leq t \leq t_{\min}, \quad (10)$$

where C_0 is the fraction of sites covered by the defects at $t=0$.

V. SIMULATION OF THE DEFECT DIFFUSION MODEL: RESULTS

A. Relaxation and scaling in strong and fragile liquids

The defect diffusion model, as presented above, has six parameters for which values must be chosen: α , T_1 , t_0 , B , T_0 , and C_D^0 . We begin with a set of parameter values which has been selected to loosely model the behavior of glycerol, i.e., $\alpha = 0.7$, $T_1 = 0$ K, $t_0 = 10^{-7}$ s, $B = 1.4379 \times 10^4$ $\text{K}^{3/2}$, $T_0 = 112.7$ K, and $C_D^0 = 2.7334 \times 10^3$. By setting T_1 to zero we ensure that the relaxation will be governed by the kinetics of defect migration. The resulting frequency dependent dissipative component of the generalized susceptibility $\chi''(\omega)$, which is related to the relaxation function $\phi(t)$ by

$$\chi''(\omega) = \omega \int_0^{\infty} \phi(t) \cos(\omega t) dt, \quad (11)$$

is presented in Fig. 1(a) for $199 \text{ K} \leq T \leq 258 \text{ K}$. Each curve is averaged over ten runs. The experimental glass transition temperature T_g for glycerol is 193 K [37].

We note the two main features of these curves. The first is the large low frequency peak, corresponding to the α relaxation, with a width roughly twice that of an exponential process. The position of this peak ω_{\max} exhibits a dramatic decrease with decreasing temperature over a narrow temperature interval of 59 K. Over this same temperature range the defect density C_D changes by four orders of magnitude. The second feature is the high frequency peak, arising from the exponential relaxation within the defects, which shows no temperature dependent shift in peak position (a result of neglecting any temperature variation of t_{\min}). This high frequency peak which emerges at $T \sim 233$ K ($C_D = 5.16\%$) does, however, display a rapid increase in its amplitude with increasing temperature. This is a reflection of the increasing contribution of the exponential relaxation below t_{\min} to the global relaxation of the system with increasing defect density. We shall refer to this peak as the β peak,

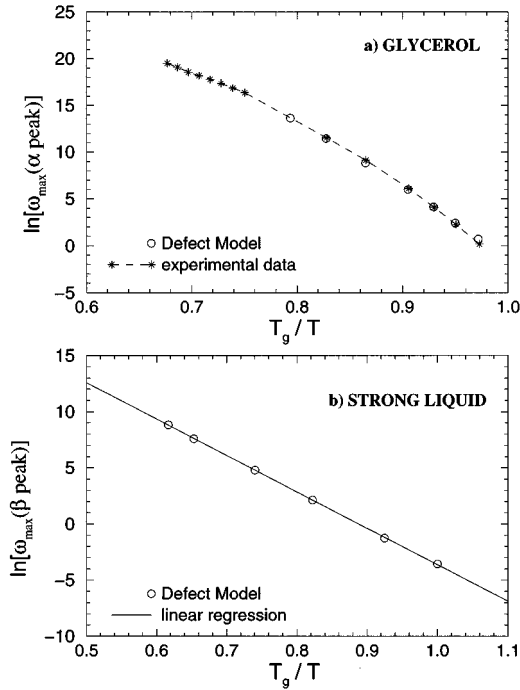


FIG. 2. (a) The position ω_{\max} of the α peak in Fig. 1(a) for the glycerol system as a function of inverse temperature in an Arrhenius plot. The experimental results from Davidson and Coles [38], and McDuffie and Litovitz [39] have been converted to angular frequencies. Notice the non-Arrhenius temperature dependence of ω_{\max} for glycerol. (b) The position ω_{\max} of the β peak in Fig. 1(b) for the strong liquid as a function of inverse temperature. The peak position now varies with an Arrhenius temperature dependence. The solid line is a linear regression through the data points. The slope of this line yields an effective activation energy of 300 kJ mol⁻¹, consistent with our choice of T_1 .

in keeping with the original definition of a similar feature by Johari [18]. Above $T=253$ K ($C_D \sim 50\%$), it becomes the dominant peak.

In Fig. 2(a) we present the temperature dependence of the α peak position ω_{\max} in an Arrhenius plot. Also included are the dielectric relaxation times from Davidson and Cole [38] and McDuffie and Litovitz [39] which have been converted to angular frequencies. The agreement between the experimental results and the model is a direct consequence of our choice for the temperature dependence of the defect density in Eq. (8).

The connection between ω_{\max} and C is demonstrated explicitly in Fig. 3 where we find the power law relation

$$\omega_{\max} \propto C^{1.58}. \quad (12)$$

Both the facilitated kinetic Ising model [1] and the defect diffusing model of Bendler and Shlesinger [12] exhibit a power law relation as well, but with different exponents. Following on from the discussion in point (2) of Sec. III, we can test whether the amplitude of the β peak is proportional to the volume fraction of fast environments. Due to the overlap of defects, this volume fraction C is a nonlinear function of the defect density C_D . In Fig. 4 we plot C (calculated directly from the simulated systems) against the β peak height and find a reasonably linear relationship until we approach

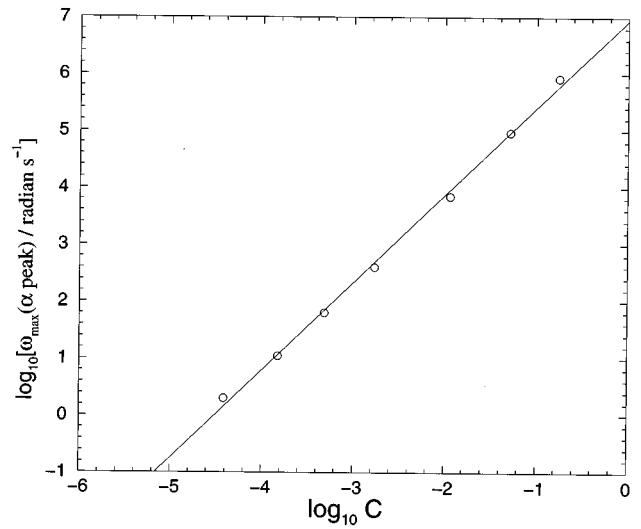


FIG. 3. The dependence of ω_{\max} of the α peak in Fig. 1(a) for glycerol on the “fast” volume fraction C . Note the approximate linearity of the log-log plot. The solid line is a linear regression through the data points with a slope of 1.58.

saturation of the system by fast environments. This dual scaling role played by C (or C_D), in establishing both the time scale of the slowest relaxation [see Eq. (12)] and the amplitude of the fastest relaxation (see Fig. 4), presents some interesting possibilities. It is possible that a scaling relationship exists between ω_{\max} and the β peak height. We have not been able to test this prediction in our simulations, however, as there is only a limited range of temperatures over which ω_{\max} and the β peak height can both be measured.

Examples of the simulated relaxation function $\phi(t)$ for glycerol at four different temperatures are shown in Fig. 5. A Kohlrausch-Williams-Watts (KWW) [40] stretched exponential function of the form

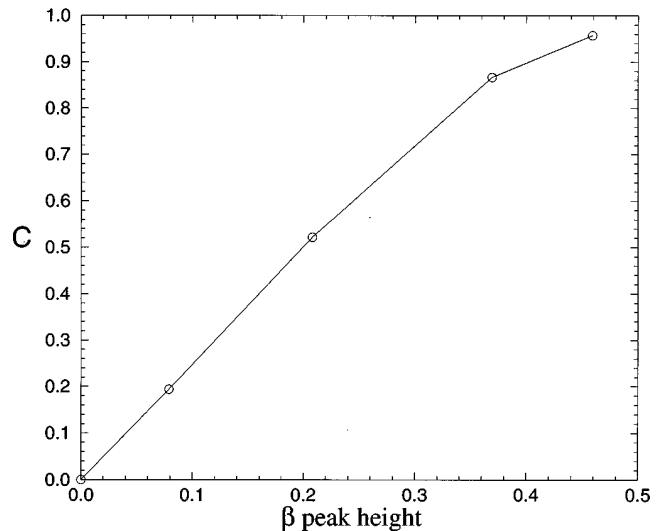


FIG. 4. The relationship between the β peak height and the “fast” volume fraction C of the glycerol system. Note the approximate linearity for all but the highest temperatures ($C \rightarrow 1$) where the system approaches saturation by the mobile regions.

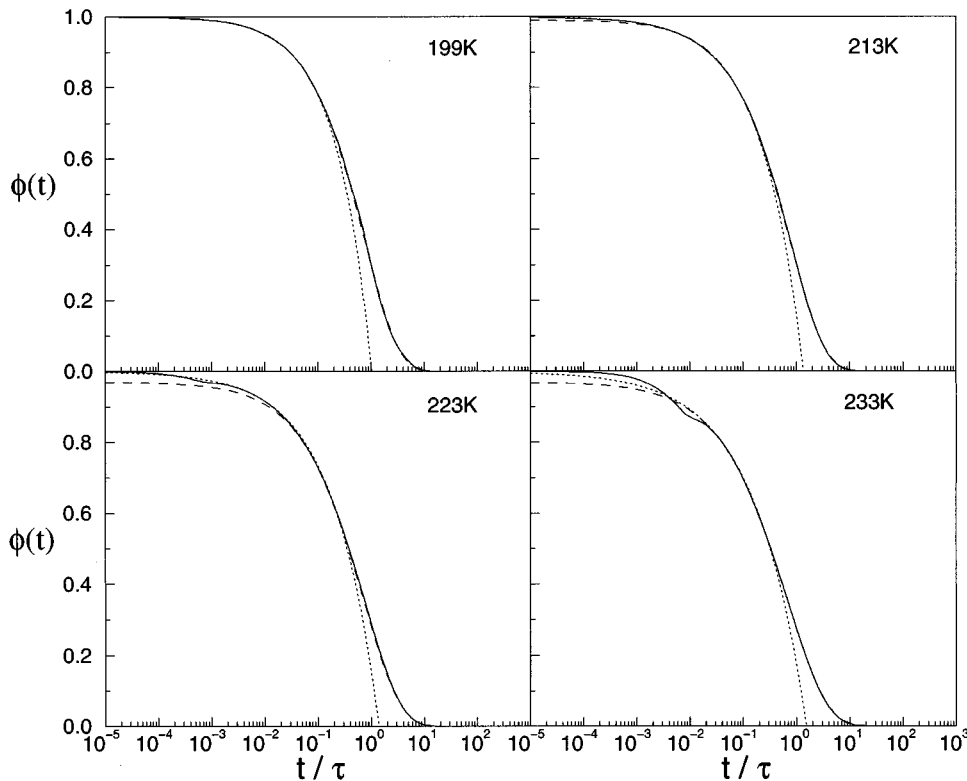


FIG. 5. The relaxation function $\phi(t)$ (solid line) for the glycerol system at four different temperatures. The “kinks” appearing in the high temperature (223 and 233 K) curves at $t=t_{\min}$ are due to the abrupt change in the relaxation mechanism at t_{\min} . Below t_{\min} , relaxation occurs exponentially within the defects but above t_{\min} , relaxation is governed solely by defect diffusion. The KWW (dashed line) and VS (dotted line) fits to $\phi(t)$ are compiled in Table I. The KWW function provides a good fit to the relaxation curves above t_{\min} , whereas the VS law is a reasonable fit only for the initial part of the α relaxation.

$$\phi(t) = A \exp[-(t/\tau_{\text{KWW}})^\gamma] \quad 0 < \gamma \leq 1, \quad (13)$$

provides a good fit to $\phi(t)$ for times greater than t_{\min} . The initial region of the α part of the relaxation can also be fitted reasonably well by a von Schweidler (VS) law [41]

$$\phi(t) = f - h(t/\tau_{\text{VS}})^b \quad 0 < b < 1, \quad (14)$$

where f is the Debye-Waller or nonergodicity factor and $h \sim 1$ is a temperature dependent material constant. We set $f=1$ and tabulate in Table I the KWW and VS fits to the relaxation functions in Fig. 5.

The analysis of Sec. III suggests that we can generate a strong liquid simply by increasing T_1 , the characteristic temperature of the “fast” relaxation time τ_f . To demonstrate this feature of the inhomogeneous picture we have set $RT_1 = 300 \text{ kJ mol}^{-1}$ (R is the gas constant) while leaving all the other parameters at their “glycerol” values, except that $t_0 = 3.7154 \times 10^{-13} \text{ s}$ and $C_D^0 = 1$. The glass transition temperature for the strong liquid is chosen to be the temperature

TABLE I. KWW: $\phi_{\text{KWW}}(t) = A \exp[-(t/\tau_{\text{KWW}})^\gamma]$ and von Schweidler (VS): $\phi_{\text{VS}}(t) = 1 - (t/\tau_{\text{VS}})^b$ fits to the relaxation function $\phi(t)$ for the “glycerol” system at four temperatures as shown in Fig. 5.

| T/K | KWW | | | VS | |
|-------|------|------------------------|----------|------------------------|------|
| | A | τ_{KWW} | γ | τ_{VS} | b |
| 199 | 1.00 | 0.496 | 0.69 | 0.665 | 0.65 |
| 213 | 0.99 | 2.046×10^{-3} | 0.67 | 3.595×10^{-3} | 0.56 |
| 223 | 0.97 | 1.029×10^{-4} | 0.63 | 2.030×10^{-4} | 0.50 |
| 233 | 0.97 | 8.133×10^{-6} | 0.58 | 1.877×10^{-5} | 0.44 |

at which $\tau = 100 \text{ s}$, a characteristic relaxation temperature which is often quoted in the literature [25]. This corresponds to $T_g = 1110 \text{ K}$ and is comparable to the glass transition temperatures of network glasses such as SiO_2 , GeO_2 , and NaAlSiO_8 [42]. The resulting susceptibility curves are plotted in Fig. 1(b) for $1110 \text{ K} \leq T \leq 1800 \text{ K}$. Now we find only a β peak whose width decreases with increasing temperature. The β peak position varies with an Arrhenius temperature dependence as illustrated in Fig. 2(b), with an effective activation energy of 300 kJ mol^{-1} which coincides with our choice of T_1 . This implies that a majority of sites in the system are relaxed exponentially within the defects below t_{\min} . Over this temperature range of 690 K the defect density varies by only 28% in contrast to the four orders of magnitude variation seen in the fragile liquid over a 59 K interval. The relaxation curves are nearly exponential and the time-temperature superposition is obeyed over the whole time range above t_{\min} .

B. On the relation between fragility and stretched relaxation

A general correlation has long been noted between the magnitude of the deviation of the relaxation time away from an Arrhenius temperature dependence (the so-called fragility) and the degree of “stretching” of the relaxation process away from a single exponential form [25,28]. Here we examine this correlation in the context of the diffusing defect model. To avoid the vagrancies of nonlinear curve fitting, we measure the degree of “stretching” of the relaxation by the interval W in $\log_{10}(t/s)$ between $\phi(t_1) = 0.01$ and $\phi(t_2) = 0.99$ at the temperature at which $\tau = 100 \text{ s}$, i.e., $W = \log_{10}(t_1/t_2)$. This width $W_{\text{exp}} = 2.661$ for an exponential function and is broader in the case of stretched exponential re-

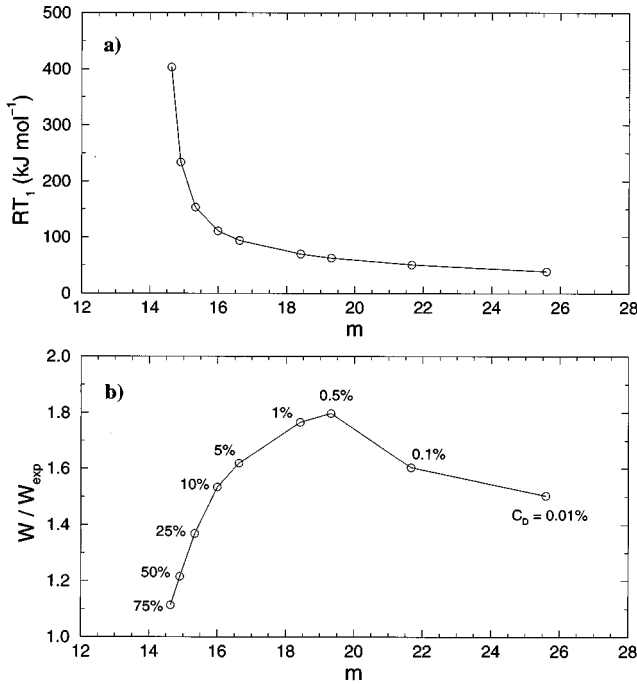


FIG. 6. (a) The variation of T_1 (the characteristic temperature of the fast Arrhenius process) with the fragility parameter m as defined in Eq. (15). (b) The width W (defined in the text) of the relaxation function $\phi(t)$ as a function of the fragility parameter m . The width W has been scaled by the exponential width $W_{\text{exp}} = 2.661$. Note the nonmonotonic relationship.

laxation. With regards to fragility, we shall follow Böhmer *et al.* [25] and define a fragility parameter m such that

$$m = \left. \frac{\partial \log_{10}(\tau)}{\partial(T_g/T)} \right|_{T=T_g}, \quad (15)$$

also evaluated at the temperature at which $\tau = 100$ s. Following the discussion in Sec. III, we shall adjust the fragility of the model by varying T_1 , the characteristic temperature of the fast Arrhenius process, while leaving the parameters which determine the temperature dependence of the defect density unchanged at the values given above. The effect of increasing T_1 is to increase the simulated T_g and hence reduce m .

The relationship between T_1 and the fragility m is shown in Fig. 6(a) and the variation of the width W with the fragility m is plotted in Fig. 6(b). As expected, W is a generally increasing function of m , but this dependence is not monotonic. The origin of this behavior appears to lie in the details of the defect dynamics applied here. As the defect density is decreased, increasingly slower aspects (longer waiting times) of the defect dynamics begin to play a significant role in the relaxation which result in an increase in W . Below $C_D \sim 0.5\%$, however, there is an effective narrowing of the relaxation time distribution associated with some intermediate time scale feature of the defect motions. This increase in W with increasing C_D at low defect densities is not well understood but could be connected to the initial appearance of the β peak in the susceptibility spectrum which leads to a

broader overall susceptibility curve. This feature is still under study.

C. Transient relaxation following temperature jumps

Inherently a nonequilibrium and nonlinear phenomenon, the transient relaxation of glass formers following a temperature jump has not received the same theoretical attention as has the temperature dependence of the relaxation time and the shape of the relaxation function. Narayanaswamy [43] has proposed a useful theory, reviewed and analyzed recently by Moynihan *et al.* [27], in which the nonlinear relaxation is described as linear relaxation occurring at a fictive temperature which, itself, is relaxing in time. The fictive temperature, which is used in this approach as an economical parametrization of nonequilibrium configurations, is assumed to relax via the same linear relaxation function. The resulting self-consistent equations reproduce the nonlinear relaxation function quite well.

In order to model transient relaxation using the diffusing defect model we must extend it to include dynamic mechanisms for defect creation and annihilation. Our model is based on the idea that defect creation or annihilation, like any other relaxation process, can only take place in the presence of a defect. From this it follows that defect creation can only take place at a site already covered by a defect. The increase in defect numbers following a temperature increase is assumed to be accomplished within the time t_{min} by adding new defects onto randomly selected existing defects until the new equilibrium defect number is reached. Microscopic reversibility requires that a defect can only be destroyed when a second defect is present. Following a temperature drop, every such binary encounter is assumed to result in the disappearance of one of the defects involved in the encounter until the new equilibrium number is reached. A more consistent picture of relaxation would incorporate the continuous fluctuation of defect numbers. We have as yet carried out only preliminary calculations for this more general model.

There is a clear kinetic asymmetry of the processes by which defect numbers change in this model. Note that while defect *numbers* can increase rapidly to a new equilibrium value, their initial *spatial* distribution is that of the existing defects and so there will be some delay until the full influence of this increase is felt by the system. A decrease in defect numbers, however, is a slower process and becomes increasingly so as the temperature (and, hence, defect density) is decreased.

In Fig. 7 we present the relaxation functions obtained immediately following temperature jumps of 5 K (both up and down) to $T = 253$ K, 233 K, and 203 K for a fragile system modeled with the ‘‘glycerol’’ parameters. The solid lines are the constant temperature T_{eq} relaxation curves, whereas the dashed lines are due to the temperature jump experiments. There are a number of interesting features in this figure. For the lowest temperature $T_{\text{eq}} = 203$ K, we see a distinct asymmetry between the relaxation functions following positive and negative temperature changes. Relaxation from the higher initial temperature ($208 \rightarrow 203$ K) is faster than from the lower temperature ($198 \rightarrow 203$ K), a consequence of the higher initial defect density in the former case. This density difference and its relatively slow relaxation via pairwise an-

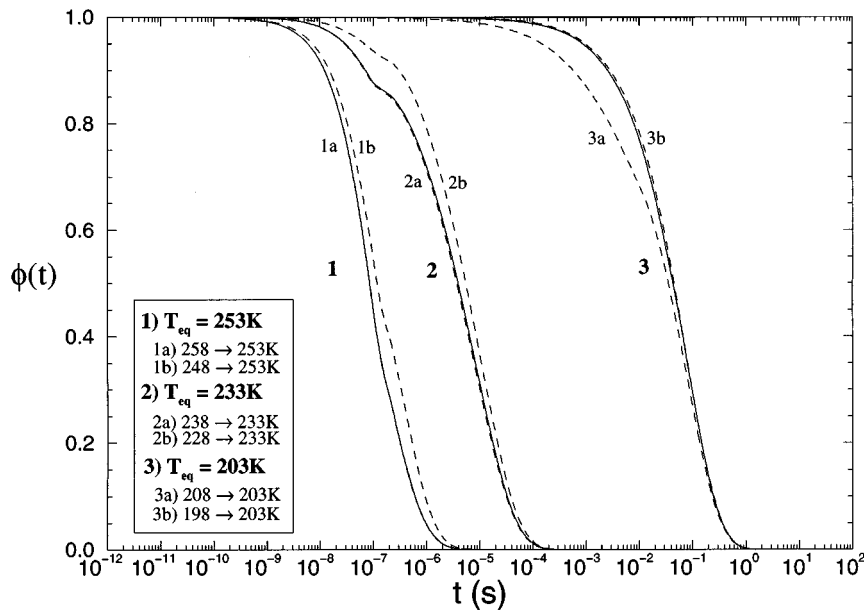


FIG. 7. The relaxation functions $\phi(t)$ for the glycerol system at three temperatures: $T_{\text{eq}} = 253$, 233, and 203 K. For each temperature, three relaxation functions are presented with different thermal histories: (a) follows a temperature jump $\Delta T = +5$ K to the final T_{eq} , (b) follows a jump $\Delta T = -5$ K to the final T_{eq} , and the third corresponds to the system equilibrated at the temperature T_{eq} . The relaxation curves following temperature jumps are given by the dashed lines, while the relaxation functions of the equilibrated systems are shown by the solid lines.

nihilation is clearly seen in Fig. 8. We also note that the system initially at 198 K exhibits a relaxation almost identical to that of the equilibrated system at 203 K. This can be rationalized as a result of the rapid *increase* in defect density permitted by this model. At low defect densities, the main relaxation mechanism is defect migration. Only a very small fraction of the system is relaxed within the defects below t_{min} . Consequently, as the initially overlapping defects in the 198 \rightarrow 203 K system start to disperse, they quickly encounter sites not already relaxed by other defects and the system rapidly equilibrates to T_{eq} .

An inversion of this effect is seen as the temperature T_{eq} is increased. At the highest temperature $T_{\text{eq}} = 253$ K, we now find that the liquid initially at the lower temperature (248 \rightarrow 253 K) relaxes significantly slower than the equilibrated liquid, in spite of the fact that the two liquids have equal defect densities. This is because at high defect densities, a major portion of the system is relaxed exponentially by the defects in their initial positions before defect diffusion takes place. Addition of new defects to the positions of pre-existing ones in the system initially at 248 K results in a lesser fraction of the system being relaxed at t_{min} . Due to the high defect density, relaxation of the whole system is completed before all the added defects are able to contribute to the relaxation process. Equilibration of the system cannot be accomplished before the entire system is relaxed. Hence the slower relaxation of the initially colder liquid. For the 258 \rightarrow 253 K temperature jump, annihilation of defect pairs occurs extremely fast, due to the high degree of defect overlap. As a result of the rapid equilibration, the relaxation curve of the initially warmer liquid is essentially identical to that of the equilibrated system.

In summary, for positive temperature jumps ($T_{\text{low}} \rightarrow T_{\text{eq}}$), equilibration becomes slower as T_{eq} is increased. The reverse is true for the negative temperature jumps ($T_{\text{high}} \rightarrow T_{\text{eq}}$). This is due to the increase in defect density and degree of overlap between defects with increasing T_{eq} . These trends have opposite effects on the relaxation of the system depending on the sign of the perturbation.

On decreasing the fragility (e.g., increasing T_1), we find relaxation taking place at higher defect densities which is less sensitive to temperature variation. As a result we observe a decrease both in the asymmetry of the transient effect and in the magnitude of the transient variation from the equilibrium relaxation. In this model, defect density provides the only system memory of thermal history.

D. Spatial correlations in relaxation kinetics

As indicated in Sec. III, the assumption that relaxation is restricted to the fast environments implies that relaxation

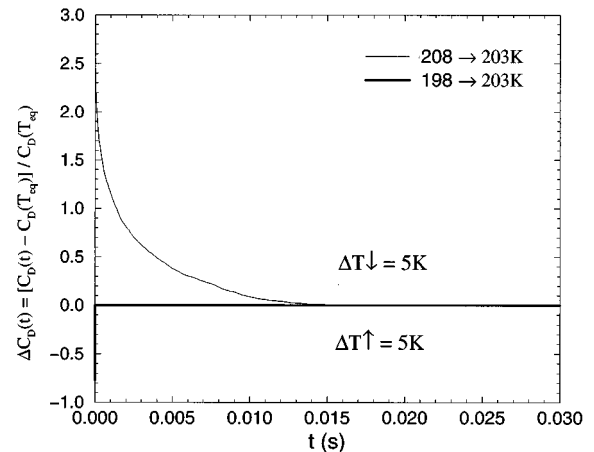


FIG. 8. The change in defect density ΔC_D for the glycerol system following a 5 K temperature jump from the initial temperature T_0 (198 and 208 K) to the final temperature T_{eq} (203 K). ΔC_D is scaled by the final defect density $C_D(T_{\text{eq}})$. Notice the slow decay of C_D to $C_D(T_{\text{eq}})$ for the system initially at the higher temperature 208 K. For the initially colder liquid, although there is an instantaneous increase in C_D to $C_D(T_{\text{eq}})$, the added defects occupy the same positions as existing defects, and so the full influence of this increase in C_D is not felt until all the extra defects have migrated away from their initial positions.

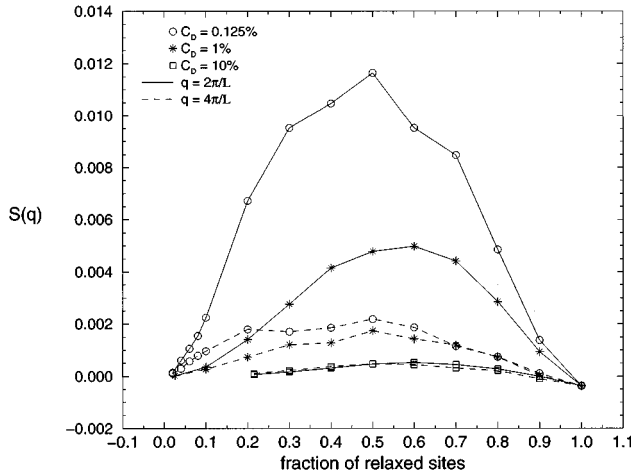


FIG. 9. Scattering from relaxed regions in the glycerol system as a function of a fraction of relaxed sites in the system for $C_D = 0.125\%$, 1% , and 10% . Note the large increase of small q scattering with a drop in C_D , indicating an increase in spatial correlations with decreasing C_D . For a specific C_D , the scattering intensity decreases with an increase in q .

must ‘‘propagate’’ out from the initial sites of relaxation. Such a process is the basis of the diffusing defect model. This requirement means that spatial correlations between different environments must become stronger as the defect density decreases. We are unaware of any previous discussion of this point. In order to quantify this correlation we have monitored the spatial distribution of the relaxation as it proceeds in time. We imagine that, as each site relaxes, its scattering cross section changes so that we can ‘‘observe’’ the following scattering function $S(q_n)$, defined as

$$S(q_n) = \frac{1}{V^2} \int_V d\mathbf{r}_1 \int_V d\mathbf{r}_2 \cos(q_n |\mathbf{r}_1 - \mathbf{r}_2|) \xi(\mathbf{r}_1) \xi(\mathbf{r}_2), \quad (16)$$

where $q_n = 2\pi n/L$ with n a positive integer, L is the length of the simulation box, and $\xi(\mathbf{r}) = 1 - \sigma(\mathbf{r})$ is the ‘‘scattering strength.’’ There is, to our knowledge, no such physical system for which *relaxation* is visible to a scattering process. $S(q_n)$ is used here to simply characterize the various complex 3D distributions of relaxed regions as a function of time.

In Fig. 9 we have plotted $S(q_n)$ for $n = 1$ and 2 calculated for systems with defect densities of $C_D = 0.125\%$, 1% , and 10% . In order to allow comparison between systems with different defect densities, $S(q_n)$ is determined at specific fractions of relaxation during the simulation runs. We note, first, that the scattering intensities are bound to go to zero at 0% and 100% relaxation, simply due to the lack of scattering contrast. Focusing on the 50% relaxation, we report the striking observation of the substantial increase in the scattering as the defect density is decreased. This scattering intensity decreases as the wave vector increases. The relaxation process at high defect densities resembles a random Poisson process in space and results in little long wavelength scattering. At lower densities the increased scattering intensities are evidence of a local ‘‘clumping’’ of relaxation about the few defects present.

VI. DISCUSSION

Central to the usefulness of kinetic inhomogeneities as an approach to understanding glassy dynamics is the question of length scales. The general picture analyzed in Sec. III allows for a range of length scales. The defect model introduces *two* length scales: one small, i.e., the radius of the defect, and one which varies with temperature, i.e., the average separation between defects. While unable to produce an absolute estimate of the density of defects, the model does indicate the variation of this characteristic length scale with temperature. In the case of the model of glycerol we find that the defect density changes by four orders of magnitude over the temperature range of 59 K, corresponding to a change in the average distance between defects by a factor of ~ 20 . The strong liquid would, in this picture, not be expected to develop a cooperative length scale much longer than that of the static structural correlations over a practical temperature range.

We have set out to accomplish two things in this paper. The first is to demonstrate that a wide range of glassy phenomena can be qualitatively accounted for as general consequences of the existence of transient kinetic inhomogeneities. These features include the relationship between strong and fragile behavior, the typical ‘‘two-step’’ relaxation function, the general correlation between fragility and the width of the relaxation function and the asymmetry of relaxation following temperature jumps. The physical picture of an inhomogeneous distribution of relaxation rates, however, leads to predictions which go well beyond simply reproducing the canonical glassy phenomenology. These features described in Sec. III include the dependence of relaxation rates on system size, the connection between the time scale of the α process and the amplitude of the β process via the volume fraction of ‘‘fast’’ regions and the different cooperative length scales in strong and fragile liquids. It is hoped that these ideas might lead to direct tests of the basic role of inhomogeneities. Some of these experimental strategies are discussed in Refs. [22] and [35].

The second aspect of this study is the presentation of a simple model representation of structural relaxation via kinetic inhomogeneities to serve as a tool to explore these strategies. We have chosen a generalized version of the diffusing defect model. The model was used to calculate the susceptibility spectra for fragile and strong liquids, the relationship between fragility and width of the relaxation process, the transient behavior of the relaxation function following temperature jumps, and the spatial distribution associated with the relaxation kinetics. We have demonstrated that the model presents a simple but quite reasonable representation of a considerable range of glassy phenomenology and provides a useful testbed for experimental concepts.

ACKNOWLEDGMENTS

It is a pleasure to thank Austen Angell for valuable encouragement and criticism. One of us (D.N.P.) gratefully acknowledges the financial support of the Henry Bertie and Florence Mabel Gritton fund.

- [1] S. Butler and P. Harrowell, *J. Chem. Phys.* **95**, 4454 (1991).
- [2] S. Butler and P. Harrowell, *J. Chem. Phys.* **95**, 4466 (1991).
- [3] M. Foley and P. Harrowell, *J. Chem. Phys.* **98**, 5069 (1993).
- [4] P. Harrowell, *Phys. Rev. E* **48**, 4359 (1993).
- [5] J. H. Gibbs and E. A. DiMarzio, *J. Chem. Phys.* **28**, 373 (1958).
- [6] G. Adam and J. H. Gibbs, *J. Chem. Phys.* **43**, 139 (1965).
- [7] S. A. Kivelson, D. Kivelson, X. Zhao, Z. Nussinov, and G. Tarjus, *Physica A* **219**, 27 (1995).
- [8] M. H. Cohen and G. S. Grest, *Phys. Rev. B* **20**, 1077 (1979); **21**, 4113 (1980); G. S. Grest and M. H. Cohen, in *Advances in Chemical Physics*, edited by I. Prigogine and S. A. Rice (Wiley, New York, 1981), Vol. 48, p. 455.
- [9] S. H. Glarum, *J. Chem. Phys.* **33**, 639 (1960).
- [10] M. F. Shlesinger and E. W. Montroll, *Proc. Natl. Acad. Sci. USA* **81**, 1280 (1984).
- [11] J. T. Bendler and M. F. Shlesinger, *J. Stat. Phys.* **53**, 531 (1988).
- [12] J. T. Bendler and M. F. Shlesinger, *J. Phys. Chem.* **96**, 3970 (1992).
- [13] C. A. Angell and K. J. Rao, *J. Chem. Phys.* **57**, 470 (1972); R. J. Speedy and P. G. Debenedetti, *Mol. Phys.* **86**, 1375 (1995).
- [14] J. Jäckle and A. Krönig, *J. Phys. Condens. Matter* **6**, 7633 (1994); **6**, 7655 (1994).
- [15] J. A. Hodgdon and F. H. Stillinger, *Phys. Rev. E* **48**, 207 (1993); **50**, 2064 (1994).
- [16] F. Fujara, B. Geil, H. Sillescu, and G. Fleischer, *Z. Phys. B* **88**, 195 (1992).
- [17] G. Tarjus and D. Kivelson, *J. Chem. Phys.* **103**, 3071 (1995).
- [18] G. P. Johari and M. Goldstein, *J. Chem. Phys.* **53**, 2372 (1970); G. P. Johari, *ibid.* **58**, 1766 (1973).
- [19] J. Y. Cavaille, J. Perez, and G. P. Johari, *Phys. Rev. B* **39**, 2411 (1989).
- [20] K. Schmidt-Rohr and H. W. Spiess, *Phys. Rev. Lett.* **66**, 3020 (1991); J. Leisen, K. Schmidt-Rohr, and H. W. Spiess, *Physica A* **201**, 79 (1993); A. Hever, M. Wilhelm, H. Zimmermann, and H. W. Spiess, *Phys. Rev. Lett.* **75**, 2851 (1995).
- [21] M. T. Cicerone and M. D. Ediger, *J. Chem. Phys.* **103**, 5684 (1995).
- [22] D. N. Perera and P. Harrowell, *J. Chem. Phys.* **104**, 2369 (1996).
- [23] P. Harrowell and D. W. Oxtoby, in *Nucleation and Crystallization in Liquids and Glasses*, edited by M. C. Weinberg, Special Issue of *Ceram. Trans.* **30**, 35 (1993).
- [24] G. H. Fredrickson and S. A. Brawer, *J. Chem. Phys.* **84**, 3351 (1986).
- [25] R. Böhmer, K. L. Ngai, C. A. Angell, and D. J. Plazek, *J. Chem. Phys.* **99**, 4201 (1993).
- [26] S. A. Brawer, *Relaxation in Viscous Liquids and Glasses* (American Ceramic Society, Columbus, OH, 1985), Chaps. 3 and 8.
- [27] M. A. deBolt, A. J. Easteal, P. B. Macedo, and C. T. Moynihan, *J. Am. Ceram. Soc.* **59**, 16 (1976); C. T. Moynihan, A. J. Easteal, M. A. deBolt and J. Tucker, *ibid.* **59**, 312 (1976).
- [28] I. M. Hodge, *Macromolecules* **16**, 898 (1983).
- [29] See Ref. [26], Chap. 3.
- [30] G. H. Fredrickson, *Ann. N.Y. Acad. Sci.* **484**, 185 (1986).
- [31] R. Moss and P. Harrowell, *J. Chem. Phys.* **101**, 9894 (1994).
- [32] M. Hurley and P. Harrowell, *Phys. Rev. E* **52**, 1694 (1995).
- [33] T. Odagaki and Y. Hiwatari, *Phys. Rev. A* **43**, 1103 (1991).
- [34] W. Kob and H. C. Andersen, *Phys. Rev. E* **51**, 4626 (1995).
- [35] M. Hurley and P. Harrowell (unpublished).
- [36] P. Bordewijk, *Chem. Phys. Lett.* **32**, 592 (1975).
- [37] N. O. Birge, *Phys. Rev. B* **34**, 1631 (1986).
- [38] D. W. Davidson and R. H. Cole, *J. Chem. Phys.* **19**, 1484 (1951).
- [39] G. E. McDuffie, Jr. and T. A. Litovitz, *J. Chem. Phys.* **37**, 1699 (1962).
- [40] R. Kohlrausch, *Pogg. Ann. Phys.* **91**, 198 (1854); G. Williams and D. C. Watts, *Trans. Faraday Soc.* **66**, 80 (1970); G. Williams, D. C. Watts, S. B. Dev, and A. M. North, *ibid.* **67**, 1323 (1971).
- [41] W. Götze and L. Sjögren, *Rep. Prog. Phys.* **55**, 241 (1992); **55**, 273 (1992).
- [42] See Ref. [26], p. 26.
- [43] O. S. Narayanaswamy, *J. Am. Ceram. Soc.* **54**, 691 (1971); R. Gardon and O. S. Narayanaswamy, *ibid.* **53**, 148 (1970).